

## REINNERVATION OF DENERVATED PARASYMPATHETIC NEURONES IN CARDIAC GANGLIA FROM *RANA PIPiens*

By STEPHEN ROPER AND BARBARA TAYLOR

*From the Departments of Anatomy and Physiology, University of Colorado  
School of Medicine, Denver, CO 80262, U.S.A.*

(Received 10 March 1981)

### SUMMARY

1. The sequence of events during reinnervation of the cardiac ganglion in the frog following interruption of the vagosympathetic nerve supply was studied with both electrophysiological and morphological techniques.
2. When cardiac ganglia were denervated by crushing the vagosympathetic nerve supply to the heart all synaptic endings on parasympathetic ganglion cells degenerated. Vacated post-synaptic densities were detected on denervated neurones for periods of at least 7 weeks.
3. The earliest signs of reinnervation were subthreshold responses evoked by stimulating the regenerating vagosympathetic trunks 2½–3 weeks after crushing the cardiac branches of the vagus nerves. Analysis of the reversal potentials of these responses indicated that these synapses were distant from the cell body.
4. At slightly longer times (4–5 weeks), regenerating synapses could be recognized on post-ganglionic axons; no synapses were detected on the neuronal perikarya at these times.
5. By 6–7 weeks following denervation, vagal synapses reinnervated neuronal perikarya as well as post-ganglionic axons. At the same time, vacated post-synaptic densities declined in number. Furthermore, vagal stimulation at this stage evoked large, suprathreshold post-synaptic potentials.
6. These studies indicate that post-ganglionic axons are the initial sites for reinnervation of parasympathetic neurones in the heart. Only some time later are neuronal perikarya reinnervated and ganglionic transmission completely restored.

### INTRODUCTION

A great deal of our understanding of the cellular mechanisms of repair after injury to the nervous system comes from studies on simple preparations. For example, over the past several decades a large amount of information has been amassed about the sequence of events which take place at the neuromuscular junction after peripheral nerve damage. The degeneration of motor nerve terminals, changes in the muscle cell post-synaptic membrane, and subsequent reinnervation of denervated fibres have been well-characterized (e.g. Letinsky, Fischbeck & McMahan, 1976; see reviews by Guth, 1968; Purves, 1976). In contrast, our knowledge about the changes which take

place after damage to neurone-neurone connexions is not as complete. The complexity of the central nervous system has precluded a detailed analysis at the cellular level comparable to what has been attained at the neuromuscular junction, and thus there are many gaps in our understanding of repair in neural tissue. For instance, although recent studies indicate that post-synaptic specializations on the membrane of target neurones remain intact after denervation and may represent sites for reinnervation under some circumstances (Sotelo, 1968; Raisman, Field, Ostberg, Iversen & Zigmund, 1974), we do not know how regenerating axons reach post-synaptic targets and at what point functional transmission commences.

The parasympathetic cardiac ganglion in the frog heart is a good model for studying synaptic interactions between nerve cells, particularly the changes in synaptic function which occur after injury (McMahan & Kuffler, 1971; Dennis, Harris & Kuffler, 1971; Roper & Ko, 1978). We have taken advantage of this preparation in a series of studies designed to investigate reinnervation of neurones after damage to their presynaptic nerve supply and to examine the ability of regenerating axons to restore their normal pattern of innervation on individual neurones (Ko & Roper, 1978; Roper & Ko, 1978). This paper focuses on the sequence of events that occurs after denervation and during the initial reinnervation of parasympathetic neurones in the cardiac ganglion. We describe where regenerating axons first establish synaptic contact with their targets and how this correlates with the return of functional synaptic transmission.

#### METHODS

*Experimental animals.* Adult *Rana pipiens* (15–40 g) of both sexes were housed at room temperature in tanks with running water. Frogs were fed meal worms or a slurry of liver powder, cod-liver oil, and multivitamins three times a week.

*Surgical operations.* Frogs were anaesthetized with tricaine methanesulphonate (100 µg/g body weight; Ethyl-m-aminobenzoate, Sigma), injected into the dorsal or ventral lymph sac. In experiments aimed at studying denervation changes, the right and left vagus nerves were exposed about 5 mm from their exit from the skull (i.e. about 20 mm from the heart) by incisions caudal to the tympanic membranes and both vagus nerves were cut or crushed there. The central ends of the severed nerves were tied into the surrounding musculature to prevent reinnervation of the heart.

To study reinnervation, both cardiac branches of the vagus nerves were exposed near their entry into the heart by cutting and retracting the sternum and overlying musculature, and were then crushed 1–2 mm from the heart. The sternum was sutured together and the wound stitched closed. Operated animals were kept for periods of up to 53 weeks. Although crushing the nerve supply close to the heart was somewhat more difficult than placing lesions more centrally (as above), regeneration of preganglionic axons was more rapid and occurred with greater consistency.

*Intracellular recordings and ionophoretic applications.* The isolated interatrial septum was transferred to a shallow recording chamber (see McMahan & Kuffler, 1971) containing a modified frog Ringer's solution (112 mM-NaCl, 2 mM-KCl, 5 mM-CaCl<sub>2</sub>, 3 mM-HEPES buffer, pH 7.2). Increased calcium was used to enhance transmitter release and improve the stability of micro-electrode penetrations. In some experiments, 2 µM-dihydroxy-β-erythroidine (Merck) was added to the bath to block post-ganglionic responses. Vagal nerve stumps were drawn into small suction stimulating electrodes mounted in the wall of the recording chamber. Cells were impaled with KCl-filled micro-electrodes having resistances of 100–300 MΩ. Signals from the micro-electrodes were fed into an electrometer which contained a feed-back circuit for passing current and recording potential changes with the same intracellular micropipette. We determined preganglionic conduction velocities by dividing the distance between the stimulating electrode and the impaled cell by the latency between the stimulus artifact and the onset of the post-synaptic response.

Acetylcholine (ACh) was applied by passing current through fine-tipped extracellular micro-electrodes filled with 2 M-ACh chloride, as previously described (Roper, 1976). To produce ACh responses which were relatively constant over a period of several minutes, the ACh electrode was positioned a few  $\mu\text{m}$  above the cell surface.

*Reversal potentials for post-synaptic responses.* To determine the reversal potential ( $E_r$ ) for synaptic responses produced by vagal stimulation and by ionophoretic application of ACh, we passed steady currents into neurones and measured the amplitudes of responses recorded at altered membrane potentials. In most instances, cells were impaled with a single recording and current-passing electrode to change the membrane potential as well as to record responses. In some experiments, however, neurones were impaled with independent current-passing and recording electrodes; the findings were equivalent and did not depend upon whether a single current/recording electrode or whether two independent electrodes were used.

Synaptic responses often could not be inverted, especially when a single current/recording electrode was used.  $E_r$  in these instances was estimated by extrapolation (e.g. Fig. 7). Synaptic reversal potentials obtained by extrapolation were similar to values obtained by direct inversion in other experiments and to values previously reported by Harris, Kuffler & Dennis (1971).

*Microscopy of ganglion cells.* Tissue was prepared for light microscopy by a zinc iodide-osmium method described in Proctor, Frenk, Taylor & Roper (1979). For electron microscopy, ganglia were prepared using methods similar to those described by McMahan & Kuffler (1971). Sections were mounted on slot grids for viewing.

To determine the number of synapses and post-synaptic densities on perikarya and on post-ganglionic axons, sections were inspected and electron micrographs taken at 12,000–24,000 $\times$ . Synaptic specializations on cell bodies were counted, by inspecting profiles of perikarya and tabulating the number of synapses and vacated post-synaptic densities per profile. A different approach was necessary to estimate the frequency of axo-axonic synapses since it was not practical to quantify their occurrence in terms of number per axonal profile. The incidence of axo-axonic synapses was calculated by scanning the tissue systematically over a large area at high magnification and scoring the number of axo-axonic synapses observed in a given section. The area that was scanned was then measured with a planimeter from low-magnification (250 $\times$ ) electron micrographs. An average area of 37,000  $\mu\text{m}^2$  was inspected on each section; values reported for the incidence of axo-axonic synapses were normalized to 10,000  $\mu\text{m}^2$ . To reduce sampling variability, the area occupied by perikarya (which differed from section to section) was subtracted from the total area scanned.

## RESULTS

The appearance of autonomic ganglion cells and of preganglionic vagal terminals in the intact cardiac ganglion of the frog has been presented in detail elsewhere (McMahan & Kuffler, 1971; Roper & Ko, 1978). On the average, seven to twelve vagal boutons can be identified on cell bodies in light microscopic preparations. Preganglionic fibres also form synapses *en passant* with axons of the ganglion cells, as described below. Plate 1A is photomicrograph of a neurone taken from a preparation stained with zinc iodide-osmium, illustrating the typical distribution of vagal boutons in a ganglion from a control animal. Vagal boutons were 1–2  $\mu\text{m}$  in diameter and contained clusters of small agranular vesicles apposed to thickenings on the presynaptic membrane. Post-synaptic membrane thickenings were juxtaposed to the presynaptic specializations. Small processes (< 1  $\mu\text{m}$  in length) occasionally projected from the ganglion cell body, and often were observed indenting the presynaptic boutons (large arrow, Plate 1B). Vagal synapses were also observed on axons of parasympathetic neurones (Plate 1C). Axo-axonic synapses on ganglion cells resembled synapses on the perikaryon.

The mean frequency of boutons on cell bodies in thin sections was 0.84  $\pm$  0.09 synapses per cell profile in control animals (mean  $\pm$  S.E.M., 350 profiles, eleven

animals). This is about equivalent to 28 synapses per  $10,000 \mu\text{m}^2$  of neuronal perikarya. In contrast, the mean incidence of axo-axonic synapses was only  $1.10 \pm 0.26$  per  $10,000 \mu\text{m}^2$  (mean  $\pm$  s.e.m., 223,555  $\mu\text{m}^2$ , six animals). These data suggest that the vagal boutons on the perikaryon contribute the bulk of synaptic input to ganglion cells. However, since the measurements are based on different volume samples of the tissue, a direct calculation of the relative contributions of axo-axonic versus axo-somatic vagal synapses cannot be made.

#### *Non-neuronal cells in the cardiac ganglion*

A prominent feature of the cardiac ganglion was the presence of satellite glial cells which ensheathed the neurones and the synaptic boutons with lamellar processes (Plates 1*B* and 2*A*). These glial processes interdigitated with preganglionic vagal fibres in the region of the axon hillock (Plate 2*A*). A prominent basal lamina separated the outermost satellite glial lamellae from extracellular space (arrows in Plates 1*B*, *C* and 2*A*). Basal lamina was not observed in the synaptic cleft nor between glial lamellae.

Preganglionic axons seen in cross sections of the vago-sympathetic nerves near the heart as well as within the cardiac ganglion were covered by Schwann cell lamellae and/or basal lamina except at points where vagal fibres came into direct contact with post-ganglionic axons. Semi-serial sections of one cell in which the axon could be followed for at least 50  $\mu\text{m}$  showed that the innervating vagal fibre and post-ganglionic axon were covered by Schwann cell lamellae and basal lamina along their entire lengths. The basal lamina was continuous with that ensheathing the satellite glial cell. Random sections taken from other specimens confirmed the continuity of the basal lamina surrounding satellite glial cells with that enveloping the Schwann cells around pre- and post-ganglionic axons.

#### *Synaptic responses in ganglion cells*

Vagal stimulation almost always evoked suprathreshold post-synaptic responses in ganglion cells (Fig. 1; cf. Dennis *et al.* 1971; Roper & Ko, 1978). A characteristic feature of suprathreshold vagal responses in ganglion cells from control animals was the large synaptic depolarization which outlasted the action potential (Fig. 1), and which is caused by residual transmitter action at vagal synapses (Dennis *et al.* 1971). Frequently, adjusting the stimulus intensity or reversing the polarity produced one or more subthreshold responses in addition to the suprathreshold one, indicating that cardiac ganglion cells received at least two or more separate vagal inputs. The conduction velocity of presynaptic axons, measured by stimulus-response latencies, was  $0.34 \pm 0.01$  m/sec (mean  $\pm$  s.e.m.; 186 inputs, seven animals).

#### *Denervation of the cardiac ganglion*

After cutting both vagus nerves, synaptic transmission began to fail within 24–48 hr, and disappeared completely by about 7 days. When synapses degenerated, transmitter release apparently deteriorated abruptly. We observed no intermediate stages of transmission failure as was also reported by Hunt & Nelson (1965). By 7 days, no synaptic boutons either on cell bodies or on axons were observed with light or electron microscopy, indicating that normally there are no intrinsic synapses in the cardiac ganglion of the frog and that bilateral vagotomy produces total denervation.

Even after vagal boutons disappeared, synaptic membrane specializations remained intact on ganglion cells. Vacated post-synaptic densities were found on axons as well as perikarya (Plate 3A, B). Although post-synaptic membrane densities were occasionally observed unopposed to vagal boutons in unoperated animals, their incidence increased markedly during the first week after vagotomy and this increase

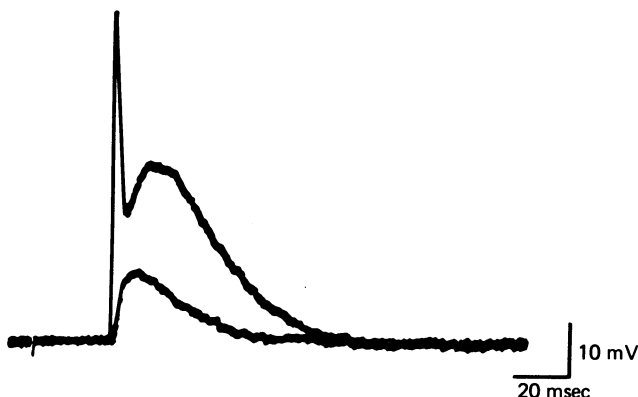


Fig. 1. Intracellular responses in a cardiac ganglion cell, evoked by stimulating the vagus nerve in an unoperated frog. The two superimposed traces illustrate a subthreshold and a suprathreshold vagal response. The two responses could be evoked separately by altering the stimulus intensity and polarity, indicating that at least two vagal preganglionic axons innervated this cell. The rising and falling phases of the action potentials in this and subsequent oscilloscope recordings were retouched.

was paralleled by the disappearance of intact vagal boutons. In unoperated animals the average length of the post-synaptic density in random thin sections was  $0.53 \pm 0.05 \mu\text{m}$  (mean  $\pm$  s.e.m.,  $n = 33$ ), but 4–21 days after vagotomy it was only  $0.31 \pm 0.02 \mu\text{m}$  ( $n = 31$ ). Inevitably, smaller denervated post-synaptic densities were more difficult to locate and may account for the finding that the number of vacated post-synaptic sites in preparations denervated for 1–3 weeks ( $0.28 \pm 0.01$  per cell profile, mean  $\pm$  s.e.m., 238 profiles, ten animals) never equalled the number of innervated sites in control ganglia ( $0.84$  synapses per cell profile).

In seven animals, vagal regeneration was prevented for up to 7 weeks to examine whether post-synaptic specializations would remain intact for long periods in the absence of presynaptic terminals (cf. Sotelo, 1968). In all cases, vacated post-synaptic densities were still observed, and their incidence ( $0.34 \pm 0.04$  per cell body profile; mean  $\pm$  s.e.m., 270 profiles) was similar to that seen 1–3 weeks after vagotomy ( $0.28$  per cell body profile).

At no period after vagotomy were there signs of trans-synaptic neuronal death or deterioration. The most apparent change in post-ganglionic cells was the aforementioned increase in the number of vacated post-synaptic sites. In contrast, satellite glial cells underwent striking changes after vagotomy; satellite glia appeared to withdraw lamellar processes, especially from the axon hillock region of ganglion cells, leaving behind large spaces filled with whorls of basal lamina (Plate 2B). The appearance of small cavities filled with basal lamina was noted occasionally in unoperated animals (cf. Pick, 1963; Uchizono, 1964; Taxi, 1976) but was never as conspicuous as in denervated ganglia. Despite the reaction of satellite glial cells to

ganglionic denervation, neuronal perikarya were not denuded since at least one or more lamellar glial processes, as well as basal lamina, remained to ensheathe the neuronal surface.

#### *Reinnervation of the cardiac ganglion*

If vagal axons were allowed to regenerate after a cardiac branch lesion, morphological signs of ganglionic reinnervation could be detected within 4–5 weeks after the operation. Regenerated synapses were initially located only on post-ganglionic axons. At this stage, profiles of cell bodies still displayed vacated post-synaptic densities. Plate 3C shows an example of a regenerated axo-axonic synapse taken from an animal in which vagal cardiac branches had been crushed 4 weeks previously. Semi-serial sections through this neurone at this stage revealed one regenerated synapse 50 µm from the perikaryon and none contacting the cell body. Regenerated axo-axonic synapses closely resembled axo-axonic contacts found in unoperated frogs. Several days later, at 6–7 weeks after crushing the vagal cardiac branches, synapses were eventually re-established on neuronal perikarya (Plate 3D). Fig. 2 compares the time course of axo-axonic reinnervation with reinnervation of the cell bodies. Furthermore, the incidence of vacated post-synaptic densities on cell bodies declined as vagal regeneration progressed, and by the end of one year, the incidence of vacated post-synaptic densities was similar to that in controls. At one year after surgery, the number and distribution of synaptic boutons on perikarya and axons were not significantly different from those in control animals (Fig. 3). In most aspects, regenerated axo-somatic synapses were similar to those in unoperated animals (Plates 1B and 3D). However, a greater proportion of regenerated axo-somatic synapses seemed to contact small projections from the perikarya during the initial stages of axo-somatic reinnervation. Regenerated preterminal axons and boutons were invested with glial lamellae, but often this investment was incomplete and portions of vagal axons directly contacted basal lamina, an infrequent occurrence in ganglia from unoperated animals.

*Restoration of functional transmission.* The first signs of functional reinnervation of the cardiac ganglion after crushing both cardiac vagal branches were recorded at about 2½–3 weeks, at times before we could reliably detect synapses in the light or electron microscope. Stimulating the regenerating vagus nerves produced small, subthreshold post-synaptic responses in ganglion cells. The conduction velocity of regenerating vagal preganglionic fibres at these early stages,  $0.28 \pm 0.01$  m/sec (mean  $\pm$  S.E.M., twenty animals, 386 neurones), was lower than normal (0.34 m/sec;  $P < 0.005$ ). At later times (6–7 weeks), at a stage corresponding to reinnervation of neuronal perikarya, suprathreshold responses with large residual depolarizations were evoked by vagal stimulation and conduction velocities had returned to control values. Fig. 4 illustrates synaptic responses recorded at two different stages of vagal reinnervation.

The proportion of ganglion cells responding to vagal stimulation rapidly increased from zero to greater than 95 % between 3 and 5 weeks after crushing the preganglionic supply (Fig. 5). By about 8 weeks, ganglionic innervation was indistinguishable from control unoperated animals.

*Initial contact of regenerating vagal axons on ganglion cells.* Intracellular responses evoked by vagal stimulation during the early stages of reinnervation were characterized by small amplitudes and slow rise times. Nevertheless, post-synaptic potentials at early stages of reinnervation occasionally elicited action potentials in ganglion cells (Fig. 6). These suprathreshold responses lacked the large residual depolarization which characterized most suprathreshold responses in intact ganglia (cf. Fig. 1). This

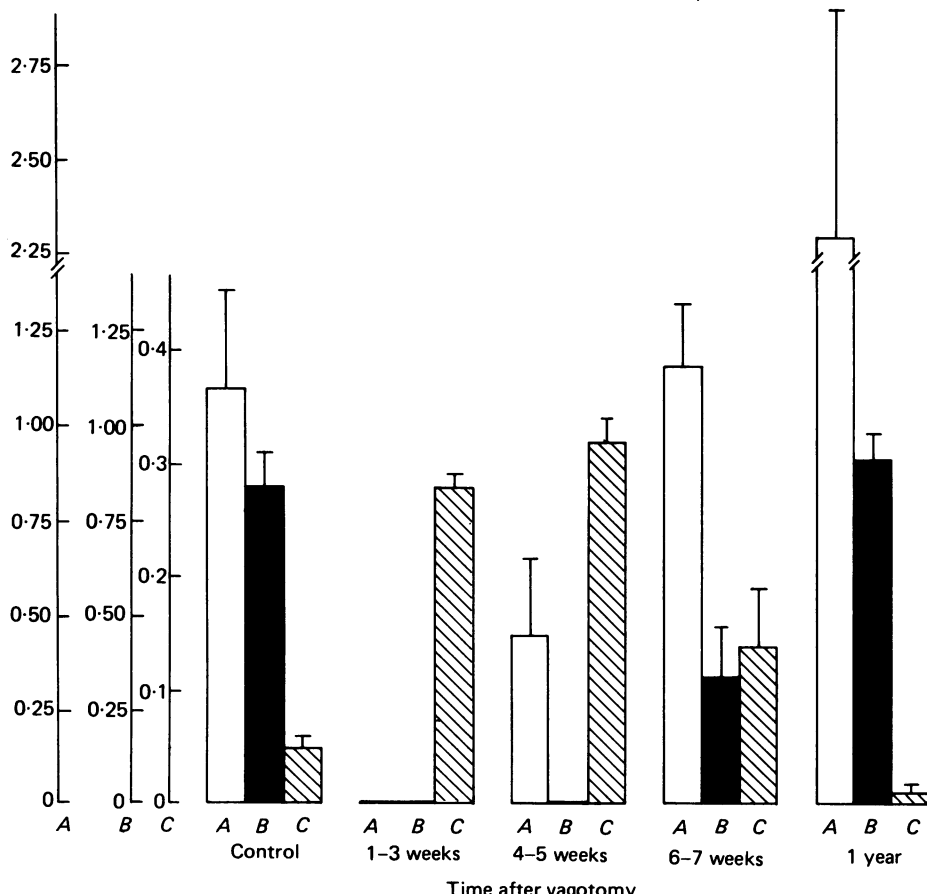


Fig. 2. Time course of vagal reinnervation of the axons and neuronal perikarya in denervated cardiac ganglia. *A*, the incidence of axo-axonic synapses in control animals ( $n = 6$ ), and in animals 1–3 weeks after bilateral vagotomy ( $n = 6$ ), 4–5 weeks after vagotomy ( $n = 5$ ), 6–7 weeks ( $n = 5$ ) and one year after vagotomy ( $n = 4$ ). *B*, the incidence of vagal boutons on perikarya in control animals ( $n = 11$ ), and 1–3 weeks after vagotomy ( $n = 10$ ), 4–5 weeks ( $n = 6$ ), 6–7 weeks ( $n = 5$ ), and one year after vagotomy ( $n = 4$ ). *C*, the incidence of vacant post-synaptic densities on perikarya in control ganglia and after bilateral vagotomy. The intervals and numbers of animals are the same as in *B*. Note that the incidence of axo-axonic reinnervation (*A*) at one year is highly variable and appears to overshoot the control values. The difference from control values, however, is not statistically significant ( $P > 0.05$ ). Scales: *A*, axo-axonic synapses per  $10,000 \mu\text{m}^2$ ; *B*, number of axo-somatic synapses per neuronal profile; *C*, number of vacant post-synaptic sites per neuronal profile.

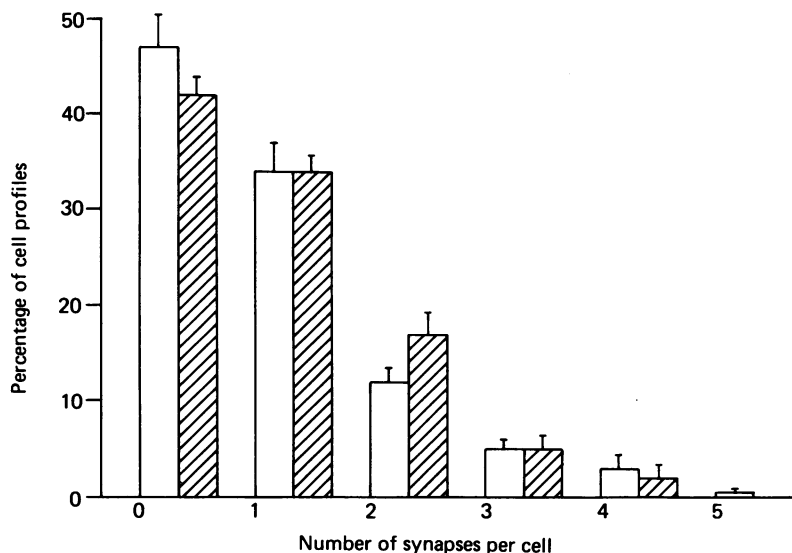


Fig. 3. Distribution of vagal boutons on cell bodies in control and reinnervated cardiac ganglia. The histogram shows the number of boutons on perikarya in electron micrographs from unoperated animals (open columns, eleven animals) and from experimental animals (hatched columns, four animals), one year after crushing the vagal nerve supply to the heart. Error bars represent S.E. of the mean.



Fig. 4. Examples of intracellular responses from reinnervated cardiac ganglion cells, evoked by stimulating the regenerating vagus nerves. *A*, vagal response recorded 5 weeks after crushing the vagus nerve. *B*, two superimposed traces illustrate subthreshold and suprathreshold vagal responses from one cell recorded 51 weeks after the operation. Vagus nerve conduction velocity in *A* was 0.20 m/sec and in *B* was 0.50 m/sec for the subthreshold response and 0.29 m/sec for the suprathreshold input.

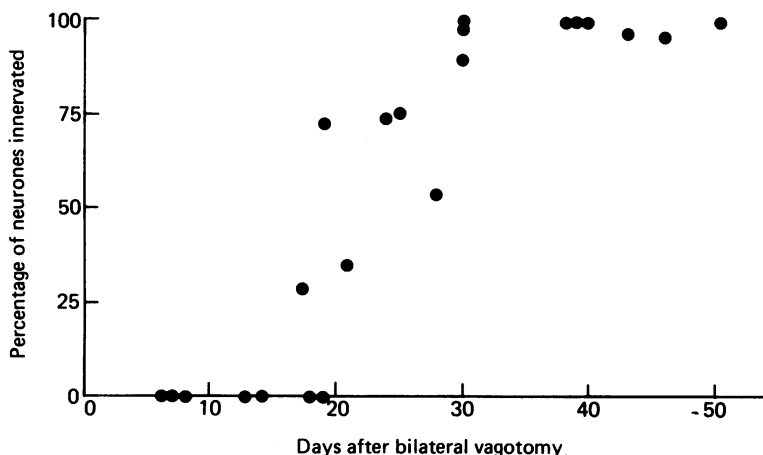


Fig. 5. The time course of reinnervation of cardiac ganglion cells after crushing the preganglionic nerve supply to the heart. Each point represents the percentage of neurones in a single ganglion in which intracellular responses were evoked by stimulating the vagus nerves, plotted as a function of time after crushing the cardiac branches of the vagus nerves. Twenty to thirty neurones were impaled in each ganglion.

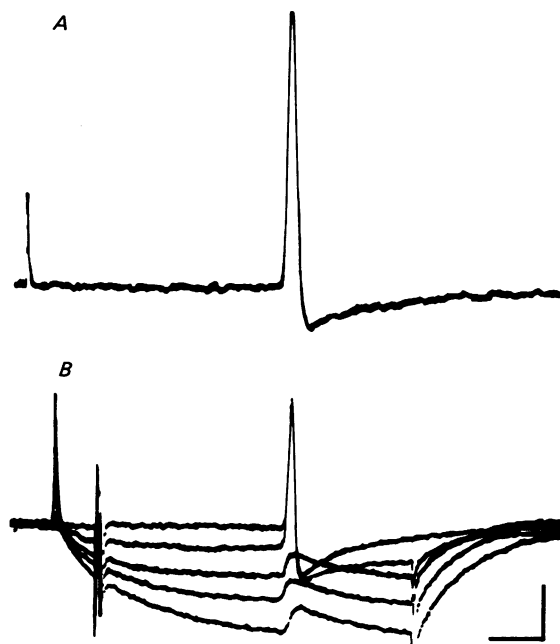


Fig. 6. An example of a suprathreshold vagal response from a reinnervated ganglion cell, caused by synaptic activity remote from the cell body. *A*, the action potential rose from the resting potential without an apparent underlying excitatory post-synaptic potential (e.p.s.p.). *B*, hyperpolarizing the cell with current pulses applied through the recording electrode blocked the action potential and revealed the small underlying e.p.s.p. The amplitude of the e.p.s.p. is only slightly affected by membrane hyperpolarization, suggesting that the site of synaptic transmission was remote. Calibrations for *A*, 10 mV, 20 msec; for *B*, 20 mV, 20 msec.

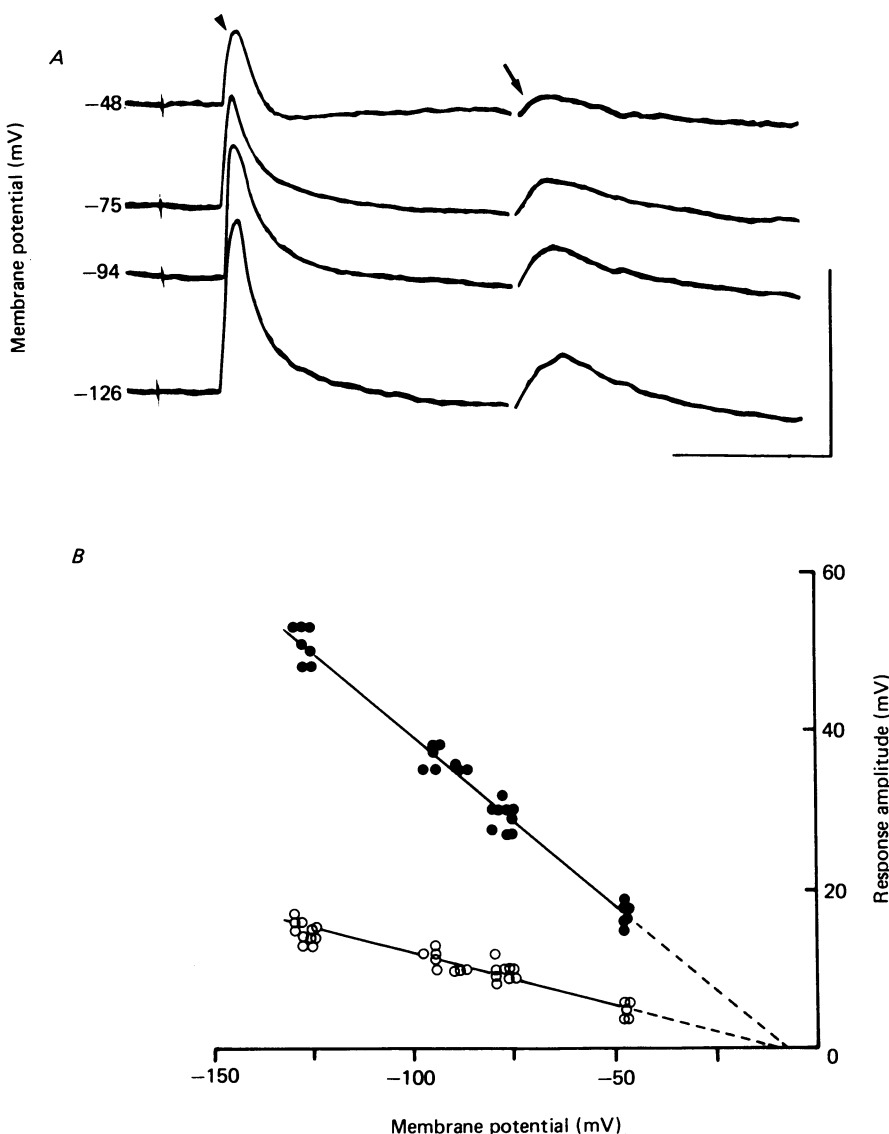
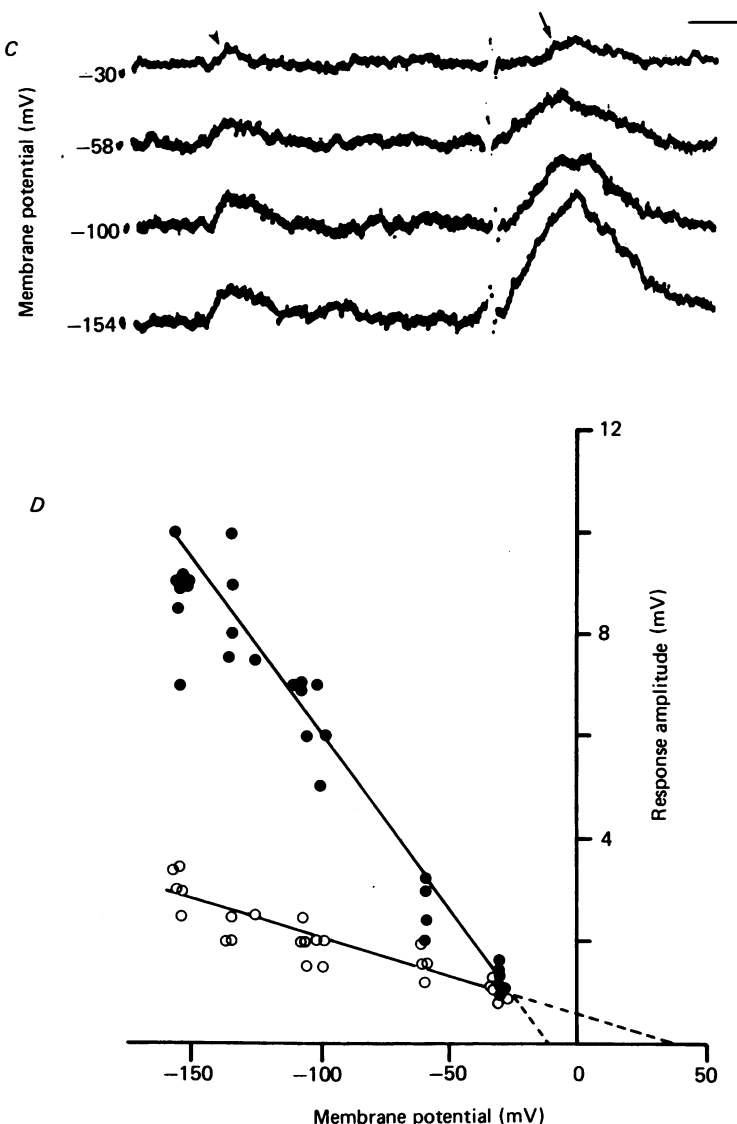


Fig. 7. Effect of ganglion cell hyperpolarization on the amplitude of synaptic responses produced by stimulating the vagus nerve and by applying acetylcholine (ACh) ionophoretically onto the neuronal perikaryon in a control animal (*A, B*) and during vagal reinnervation (*C, D*). *A*, vagal responses (arrow head) were reduced to subthreshold levels by  $2 \mu\text{M}$ -dihydroxy- $\beta$ -erythroidine and are followed by responses to ACh (arrow), applied ionophoretically by a 2 msec current pulse of constant amplitude. The top trace was recorded at the membrane resting potential ( $-48 \text{ mV}$ ) and lower traces were recorded while the membrane was hyperpolarized to the indicated values by constant currents applied through the recording electrode. Calibrations = 50 mV, 100 msec. *B*, the amplitudes of the vagal responses (filled circles) and of the ACh responses (open circles) from the cell shown in *A* are plotted as a function of the membrane potential. Linear regression lines



are drawn through the points ( $r^2$  for vagal responses = 0.98 and for ACh responses = 0.94). The dashed lines are extrapolations to the reversal potential,  $E_r$ , for each response.  $E_r$  for vagal responses (-7.2 mV) is similar to that for ACh (-9.2 mV). C, intracellular recordings of a remote vagal input (arrow head), and of ACh responses (arrow). Traces were recorded while the membrane was polarized as indicated. The vagus nerves had been crushed 5 weeks prior to the experiment. Calibrations = 5 mV, 20 msec. D, the amplitudes of the vagal responses (open circles) and the ACh responses (filled circles) are plotted as a function of membrane potential. Linear regression lines are drawn through the points ( $r^2$  for vagal responses = 0.85 and for ACh responses = 0.96). The dashed lines are extrapolations to the reversal potential,  $E_r$ , for each response.  $E_r$  for the regenerated vagal input = +36.1 mV and for the ACh responses = -11.6 mV.

observation, along with the small amplitudes and slow rise times of subthreshold responses, suggested that at early stages of reinnervation, synaptic inputs were remote from the perikaryon. This corroborated the morphological findings. To test this further we examined whether there were discrepancies between the apparent reversal potentials for regenerated vagal responses, compared with responses produced

TABLE 1. Reversal potentials ( $E_r$ ) for remote, regenerating vagal responses and for ACh responses at the cell body, 3–5 weeks after crushing the vagus nerve

| Experiment | Resting potential (mV) | Nerve      |       | ACh        |       | Difference (mV):<br>$E_r(\text{nerve}) - E_r(\text{ACh})$ |
|------------|------------------------|------------|-------|------------|-------|---|
|            |                        | $E_r$ (mV) | $r^2$ | $E_r$ (mV) | $r^2$ |   |
| 1          | -40                    | +11.3      | 0.45  | -10.6      | 0.99  | +21.9   |
| 2          | -40                    | +101.0     | 0.41  | -19.6      | 0.89  | +120.6  |
| 3          | -43                    | +12.6      | 0.77  | -9.1       | 0.97  | +21.7   |
| 4          | -53                    | -2.9       | 0.44  | -32.8      | 0.85  | +29.9   |
| 5          | -40                    | -14.0      | 0.89  | -14.3      | 0.96  | +0.3  |
| 6          | -33                    | -10.4      | 0.91  | +0.9       | 0.97  | -9.5  |
| 7          | -30                    | +36.1      | 0.85  | -11.6      | 0.96  | +47.7   |
| 8*         | -35                    | +9.6       | 0.70  | -13.7      | 0.99  | +23.3   |
| 9*         | -42                    | -13.3      | 0.93  | -21.1      | 0.96  | +7.8  |
| 10         | -40                    | +56.3      | 0.49  | +4.1       | 0.89  | +52.2   |
| 11         | -50                    | -34.0      | 0.90  | -42.6      | 0.96  | +8.6  |
| Mean =     | -41                    | +13.9      |       | -15.5      |       | +29.5   |
| S.E.M. =   | ±2                     | ±11.5      |       | ±4.1       |       | ±10.7   |

Cells were impaled with single current/recording electrodes or with independent current-passing and recording micropipettes. ACh was applied ionophoretically to the neuronal perikaryon via an extracellular micropipette.  $E_r$  was obtained in each case by extrapolating the graph of response versus membrane potential (see Fig. 7). The correlation coefficient,  $r^2$ , for each graph is included. The differences (last column) between reversal potentials for nerve-evoked responses (column 3) and ACh potentials (column 5) are significant at the 0.005 level (Wilcoxon Rank Pair Test).

\* Cell impaled with independent current/recording micropipettes.

by applying acetylcholine (ACh) directly onto neuronal perikarya. The reversal potential ( $E_r$ ) in unoperated animals for nerve-evoked and for ACh responses, when both were generated at the cell body, was identical and was between -20 mV and 0 mV (Fig. 7A, B), as previously reported by Dennis *et al.* (1971). Fig. 7C shows nerve-evoked and ACh potentials recorded at different membrane potentials at an early stage of reinnervation. Fig. 7D shows the amplitudes of the responses plotted against the membrane potential. In contrast to the similarity of reversal potentials for vagal and ACh responses in control ganglia, reversal potentials were +36.1 mV and -11.6 mV for nerve-evoked and ACh responses, respectively, for this neurone. The average  $E_r$  for ACh responses in experimental animals during early stages of reinnervation was  $-15.5 \pm 4.1$  mV, (mean ± S.E.M.,  $n = 11$ ) and did not differ from ACh responses in control, innervated ganglia ( $-12.1 \pm 2.0$  mV,  $n = 5$ ; cf. Dennis *et al.* 1971).

Table 1 summarizes data comparing  $E_r$  for regenerating nerve-evoked and ACh responses from several experiments 3–5 weeks after vagotomy. These data illustrate that the mean  $E_r$  of nerve-evoked responses (+13.9 mV) in reinnervated ganglia was significantly more positive than that for ACh responses at the cell body (-15.5 mV).

At later stages of reinnervation (6–7 weeks) when vagal stimulation evoked large suprathreshold post-synaptic potentials and when vagal synapses had begun to reinnervate neuronal perikarya, reversal potentials for nerve-evoked responses were indistinguishable from those in intact ganglia. If one assumes that nerve-released and ionophoretically applied transmitter produce the same post-synaptic conductance changes whether acting on the axon or the perikaryon, then the discrepancies in apparent reversal potentials reported here are produced by electrotonic decrement of synaptic responses generated remote from the current-passing and recording electrodes. In brief, these findings indicate that at early stages of vagal reinnervation (3–5 weeks), synaptic contact is established at some distance from the perikaryon and only later (6+ weeks) is the soma reinnervated.

In control animals we measured reversal potentials for subthreshold vagal responses to determine whether they differed from reversal potentials for suprathreshold vagal inputs. The apparent reversal potentials for subthreshold responses were consistently positive (mean  $\pm$  s.e.m. =  $+36.8 \pm 16.8$  mV,  $n = 6$ ), indicating that subthreshold vagal responses may originate from synapses remote from the perikaryon even in control, unoperated animals. Cardiac ganglion cells in the frog normally are multiply innervated, but typically one of the vagal inputs is suprathreshold and all remaining inputs are subthreshold (cf. Figs. 1 and 4). Thus, the above findings suggest that only one vagal preganglionic ending, the suprathreshold one, innervates the cell body in intact ganglia and other vagal inputs are limited to axonal sites.

#### DISCUSSION

The main objectives of this study have been to describe the changes which take place in the parasympathetic cardiac ganglion of the frog after its nerve supply has been interrupted, and to characterize the early stages of reinnervation. An important finding from this study is that regenerating axons first re-establish functional synaptic contact on the axons of their target neurones long before the neuronal perikaryon is reinnervated, and that these remote inputs can sometimes excite the neurones. Furthermore, there were discrepancies between the times at which the first evidence for reinnervation could be detected morphologically compared with when it could be observed physiologically. The latter can be explained by the fact that axo-axonic synapses were few in number and relatively difficult to locate. In contrast, post-synaptic potentials in the cell body can be recorded even if the synapse is remote, and thus they were readily detected. The caveat learned from these observations is that studying the pattern of synaptic innervation in nervous tissue, especially during regeneration, may be quite misleading unless the possibility of remote innervation is taken into account and unless structure and function are correlated.

#### *Reaction of ganglion cells and glia to denervation*

Relatively few changes in the morphology of ganglion cells were observed after denervation. For example, vacated post-synaptic specializations remained intact, although smaller in size, for long periods in the absence of presynaptic input. These findings corroborate those of Sotelo (1968) who studied denervation in sympathetic ganglia from *R. pipiens*. In *R. esculenta*, however, Taxi (1979) reported that

post-synaptic specializations on sympathetic neurones did not remain for long periods after denervation.

The reaction of satellite glial cells to denervation, however, was striking. The withdrawal of glial processes left large empty spaces containing whorls of basal lamina. In intact ganglia, a single layer of basal lamina enveloped the outermost lamella of satellite glia cells and thus the appearance of whorls of basal lamina, apparently in interlamellar spaces left behind by retracting glial processes, may represent newly synthesized material. The complex arrangement of glial trabeculae and basal lamina surrounding empty spaces in intact, innervated amphibian autonomic ganglion cells has been reported by Pick (1963), Uchizono (1964), and Taxi (1976) but was only occasionally observed in our material and was never as pronounced as after denervation. The change in the appearance of satellite glia after ganglionic denervation is similar to the reaction of glial cells in damaged peripheral nerves. After peripheral nerve injury, Schwann cells retract their processes and divide, leaving behind empty spaces surrounded by basal lamina (Nathaniel & Pease, 1963; Thomas, 1964).

The surface of denervated ganglion cells was never exposed directly to extracellular space. In rare instances when gaps were observed in the satellite glial covering, the basal lamina remained as a continuous layer. The basal lamina appeared to provide an unbroken envelope investing each neurone, its satellite glial cells, the pre- and post-ganglionic axons, and their surrounding Schwann cells. Thus, the basal lamina could act as a continuous scaffolding (cf. Vracko, 1978), or guide, for regenerating preganglionic axons, possibly directing their regrowth all the way from the site of the vagal lesion to their targets in the cardiac ganglion.

#### *Reinnervation of ganglion cells*

The findings that the disappearance of vacated post-synaptic thickenings coincided with the return of vagal innervation during regeneration suggests that pre-existing synaptic sites were re-occupied during reinnervation. Similar observations were made by Raisman and his colleagues in decentralized mammalian sympathetic ganglia (Raisman *et al.* 1974). In tissues such as denervated muscle, where reinnervation can be followed more directly, it is well established that post-synaptic specializations remain intact long after presynaptic terminals have degenerated, and that these specializations are specific targets for reinnervation (Letinsky *et al.* 1976; cf. Sanes, Marshall & McMahan, 1978). The precision with which denervated end-plates are reinnervated by regenerating motor axons is striking. By analogy, it is reasonable to conclude that reinnervation of neurones may also take place at pre-existing post-synaptic specializations. Vacated post-synaptic thickenings may not, however, be a prerequisite for reinnervation in all circumstances; for example, after axotomy, presynaptic boutons withdraw and vacated post-synaptic densities are greatly reduced; nevertheless reinnervation occurs (Purves, 1975; Matthews & Nelson, 1975; Purves & Thompson, 1979; Taxi, 1979).

Synaptic contact during the initial stages of reinnervation in the cardiac ganglion, albeit remote from the cell body, may nevertheless have profound effects at the neuronal perikaryon. For example, the density of transmitter receptors on the membrane surface at the cell body may be controlled in part by reinnervation at distal

axo-axonic sites. That is, the entire neuronal perikaryon of denervated ganglion cells, including both synaptic and extrasynaptic regions, is exquisitely sensitive to ionophoretically applied acetylcholine, (Kuffler, Dennis & Harris, 1971; Roper, 1976), a phenomenon called 'denervation supersensitivity'. Dennis & Sargent (1979) recently reported that the ACh supersensitivity at the cell body in cardiac ganglion cells disappeared very early during vagal reinnervation in the frog, at stages corresponding to those in the present studies where only axo-axonic synaptic contact occurs. It may be that other properties of denervated neuronal perikarya, in addition to membrane chemosensitivity, are altered by re-occupation of remote, axo-axonic synaptic sites during regeneration.

We would like to extend our thanks to Drs A. R. Martin, D. Purves, W. Proctor, N. McKenna, and P. Sargent for a critical reading of the manuscript and to Dr S. Frenk for assistance during the experiments. We are indebted to Betty Aguilar, Sharon Ferdinandsen and Judy Paden for their expert secretarial assistance. This work is supported by grants from the Colorado Heart Association, the American Heart Association, and USPHS NS11505 and NS00257.

#### REFERENCES

- DENNIS, M. J., HARRIS, A. J. & KUFFLER, S. W. (1971). Synaptic transmission and its duplication by focally applied acetylcholine in parasympathetic neurons in the heart of the frog. *Proc. R. Soc. B* **177**, 509–539.
- DENNIS, M. J. & SARGENT, P. B. (1979). Loss of extrasynaptic acetylcholine sensitivity upon reinnervation of parasympathetic ganglion cells. *J. Physiol.* **289**, 263–275.
- GUTH, L. (1968). 'Trophic' influences of nerve on muscle. *Physiol. Rev.* **48**, 645–687.
- HARRIS, A. J., KUFFLER, S. W. & DENNIS, M. J. (1971). Differential chemosensitivity of synaptic and extrasynaptic areas on the neuronal surface membrane in parasympathetic neurones of the frog, tested by microapplication of acetylcholine *Proc. R. Soc. B* **177**, 541–553.
- HUNT, C. C. & NELSON, P. G. (1965). Structural and functional changes in the frog sympathetic ganglion following cutting of the presynaptic nerve fibres. *J. Physiol.* **177**, 1–20.
- KO, C.-P. & ROPER, S. (1978). Disorganized and 'excessive' reinnervation of frog cardiac ganglia. *Nature, Lond.* **274**, 286–288.
- KUFFLER, S. W., DENNIS, M. J. & HARRIS, A. J. (1971). The development of chemosensitivity in extrasynaptic areas of neuronal surface after denervation of parasympathetic ganglion cells in the heart of the frog. *Proc. R. Soc. B* **177**, 555–563.
- LETINSKY, M. S., FISCHBECK, K. H. & McMAHAN, U. J. (1976). Precision of reinnervation of original postsynaptic sites in frog muscle after a nerve crush. *J. Neurocytol.* **5**, 691–718.
- McMAHAN, U. J. & KUFFLER, S. W. (1971). Visual identification of synaptic boutons on living ganglion cells and of varicosities in postganglionic axons in the heart of the frog. *Proc. R. Soc. B* **177**, 485–508.
- MATTHEWS, M. & NELSON, V. H. (1975). Detachment of structurally intact nerve endings from chromatolytic neurones of rat superior cervical ganglion during the depression of synaptic transmission induced by post-ganglionic axotomy. *J. Physiol.* **245**, 91–135.
- NATHANIEL, E. J. H. & PEASE, D. C. (1963). Collagen and basement membrane formation by Schwann cells during nerve regeneration. *J. Ultrastruct. Res.* **9**, 550–560.
- PICK, J. (1963). The submicroscopic organization of the sympathetic ganglion in the frog (*Rana pipiens*). *J. comp. Neurol.* **120**, 409–462.
- PROCTOR, W., FRENK, S., TAYLOR, B. & ROPER, S. (1979). 'Hybrid' synapses formed by foreign innervation of parasympathetic neurons: a model for selectivity during competitive reinnervation. *Proc. natn. Acad. Sci., U.S.A.* **76**, 4695–4699.
- PURVES, D. (1975). Functional and structural changes in mammalian sympathetic neurones following interruption of their axons. *J. Physiol.* **252**, 429–463.
- PURVES, D. (1976). Long term regulation in the vertebrate peripheral nervous system. In *International Review of Physiology, Neurophysiology II*, vol. 10 ed. PORTER, R. Baltimore: University Park Press.

- PURVES, D. & THOMPSON, W. (1979). The effects of post-ganglionic axotomy on selective synaptic connexions in the superior cervical ganglion of the guinea-pig. *J. Physiol.* **297**, 95–110.
- RAISMAN, G., FIELD, P. M., OSTBERG, A. J. C., IVERSEN, L. L. & ZIGMOND, R. E. (1974). A quantitative ultrastructural and biochemical analysis of the process of reinnervation of the superior cervical ganglion in the adult rat. *Brain Res.* **71**, 1–16.
- ROPER, S. (1976). The acetylcholine sensitivity of the surface membrane of multiply-innervated parasympathetic ganglion cells in the mudpuppy before and after partial denervation. *J. Physiol.* **254**, 455–473.
- ROPER, S. & KO, C.-P. (1978). Synaptic remodeling in the partially denervated parasympathetic ganglion in the heart of the frog. In *Neuronal Plasticity*, ed. COTMAN, C. W. New York: Raven Press.
- SANES, J. R., MARSHALL, L. M. & McMAHAN, U. J. (1978). Reinnervation of muscle fibres basal lamina after removal of myofibres. *J. Cell Biol.* **78**, 176–198.
- SOTELO, C. (1968). Permanence of postsynaptic specializations in the frog sympathetic ganglion cells after denervation. *Expl. Brain Res.* **6**, 294–305.
- TAXI, J. (1976). Morphology of the autonomic nervous system. In *Frog Neurobiology*, ed. LLINAS, R. & PRECHT, W. Berlin, Heidelberg, New York: Springer-Verlag.
- TAXI, J. (1979). Degeneration and regeneration of frog ganglionic synapses. *Neuroscience* **4**, 817–823.
- THOMAS, P. K. (1964). The deposition of collagen in relation to Schwann cell basement membrane during peripheral nerve regeneration. *J. Cell Biol.* **23**, 375–382.
- UCHIZONO, K. (1964). On different types of synaptic vesicles in the sympathetic ganglia of amphibia. *Jap. J. Physiol.* **14**, 210–219.
- VRACKO, R. (1978). Anatomy of basal lamina scaffold and its role in maintenance of tissue structure. In *Biology and Chemistry of Basement Membranes*, ed. KEFALIDES, N. A. New York: Academic Press.

#### EXPLANATION OF PLATES

##### PLATE 1

*A*, example of a cardiac ganglion cell from an unoperated animal. The ganglion was stained with zinc iodide-osmium and whole-mount embedded. Vagal terminals are darkly stained while the parasympathetic neurone and its axon are only faintly stained. The vagal preganglionic axon forms an axo-axonic contact (arrow) and deposits a number of boutons at the axon hillock of the ganglion cell. Calibration = 10 µm.

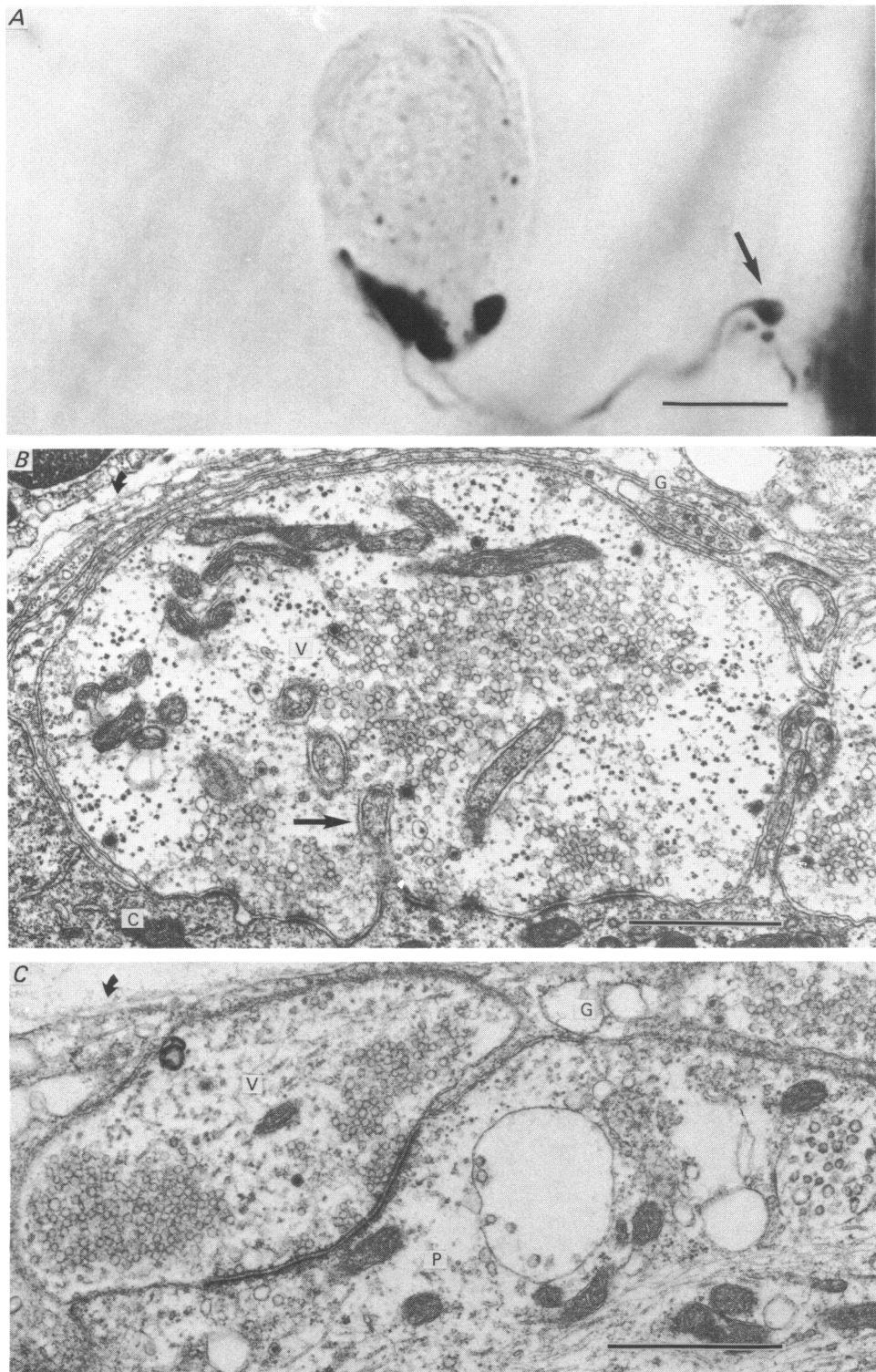
*B*, an electronmicrograph of a vagal bouton (V) contacting a cardiac ganglion cell (C). The post-synaptic membrane often exhibits small protuberances, or thorns (arrow), as shown here. Lamellar glial cell processes (G) cover the bouton and a basal lamina (curved arrow) lies outside the glial encapsulation. Calibration = 1 µm.

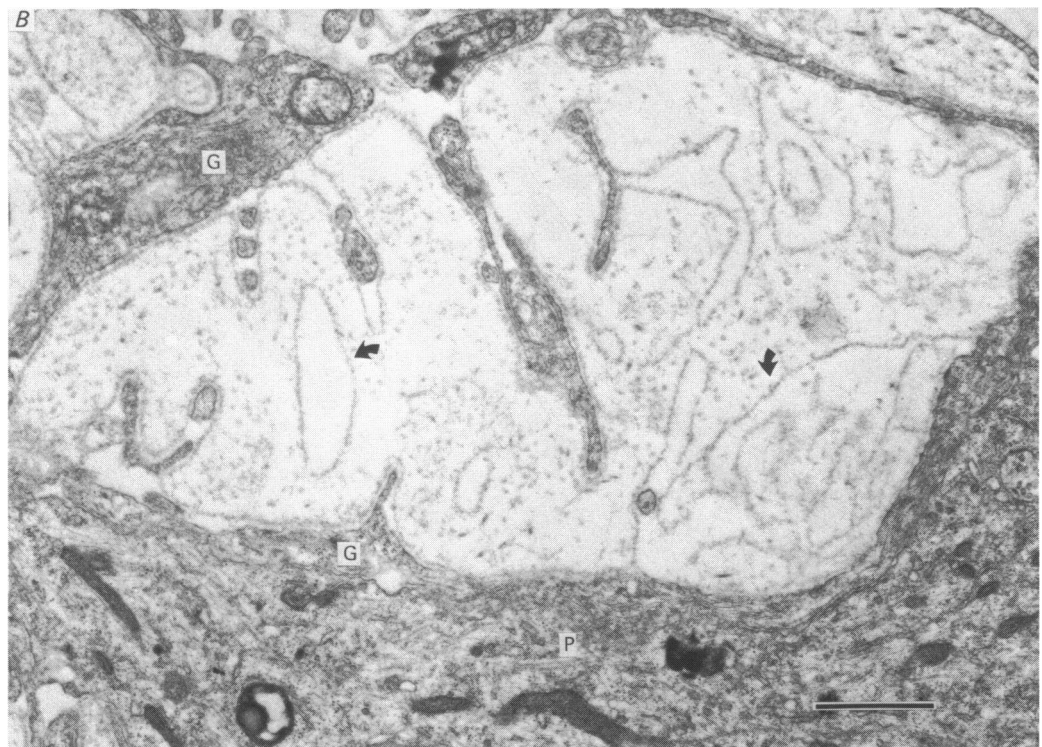
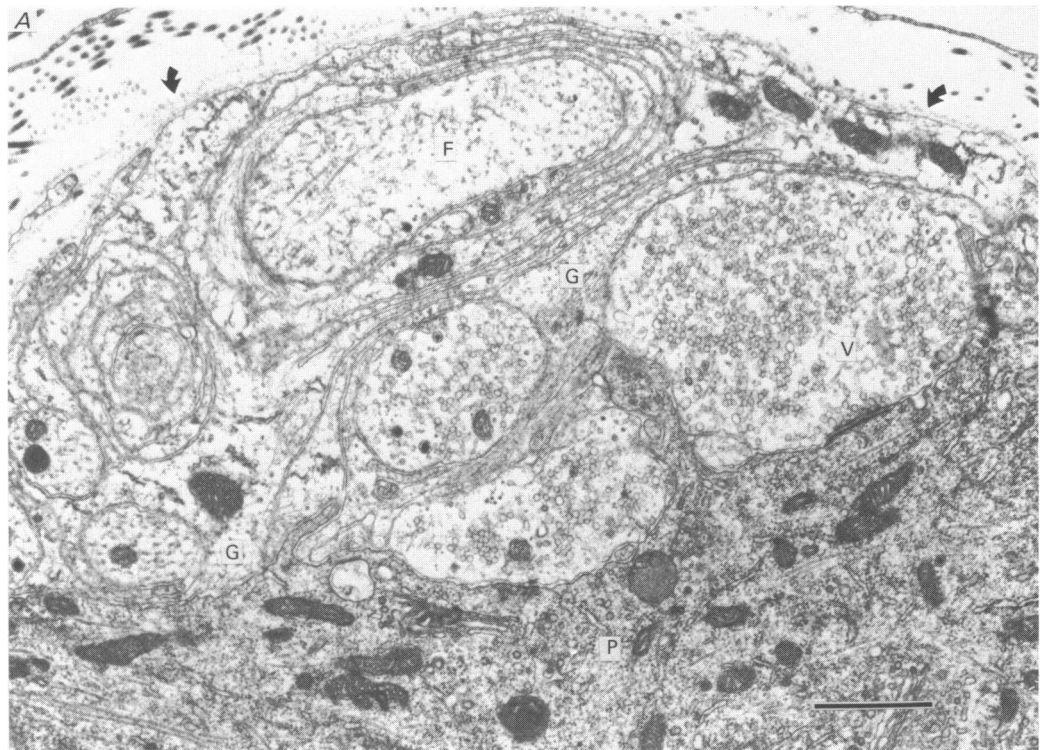
*C*, an electron micrograph of an axo-axonic synapse. A vagal terminal (V) contacts a post-ganglionic axon (P) remote from its parent cell body. Numerous synaptic vesicles are found in the presynaptic vagal terminal, and are associated with pre- and post-synaptic membrane densities. Glial cell lamellae (G) cover the post-ganglionic axon. A basal lamina (curved arrow) lies outside the glial investment. Calibration = 1 µm.

##### PLATE 2

*A*, an electron micrograph of the axon hillock region of a cardiac ganglion cell in a control animal. Preganglionic vagal fibres (F) spiral around the axon hillock and terminate in synaptic boutons (V). Glial processes (G) interdigitate among and surround the vagal fibres and cover the post-ganglionic axon (P). Basal lamina (curved arrows) covers the external surface of the glial processes.

*B*, an electronmicrograph of the axon hillock region of a denervated ganglion cell, 10 days after bilateral vagotomy. Vagal fibres and boutons have degenerated and the glial processes (G) have withdrawn from the hillock region, leaving behind whorls of basal lamina (curved arrows). Even though most glial processes have withdrawn from the region, the post-ganglionic axon (P) remains covered by one or more glial lamellae. Calibration for *A*, *B* = 1 µm.





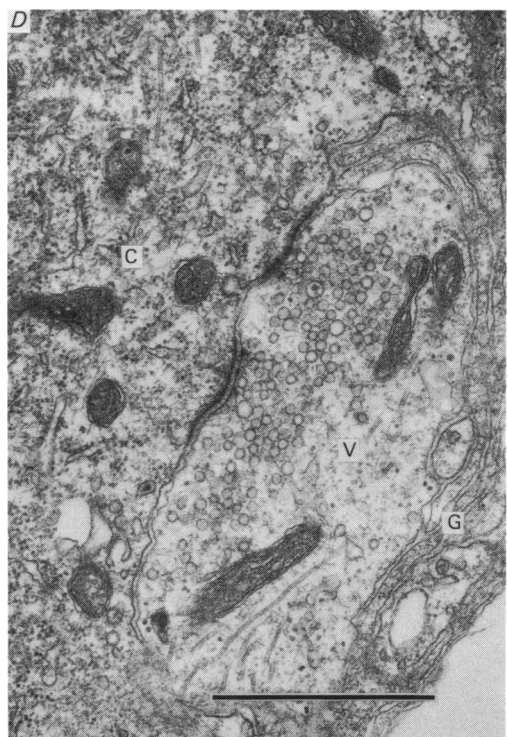
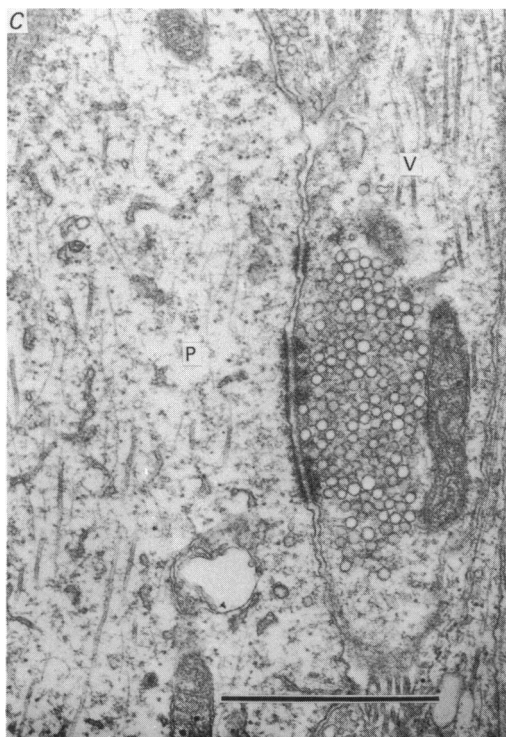
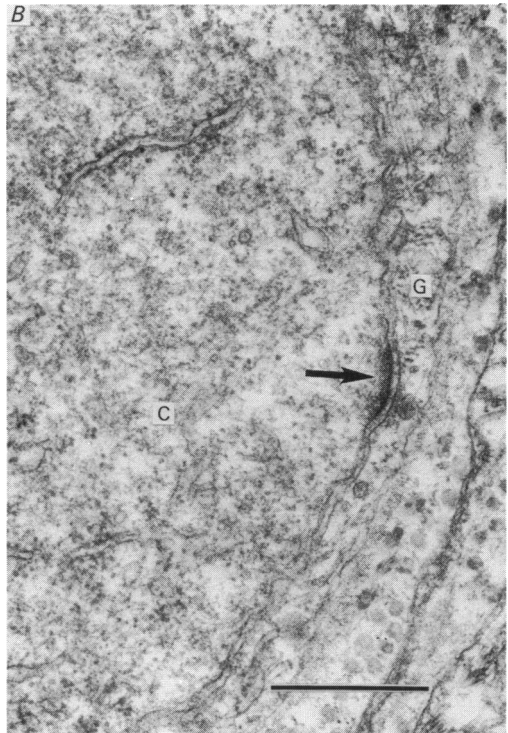
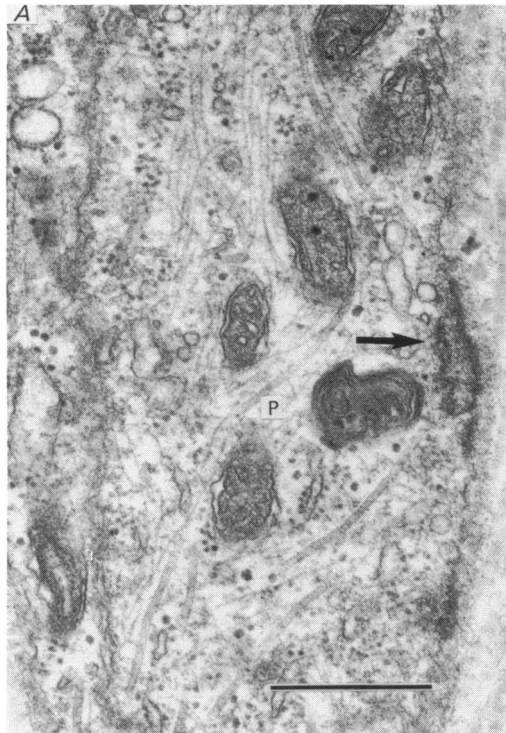


## PLATE 3

Electron micrographs of denervated cardiac ganglion cells.

*A*, an example of a vacated synaptic site (arrow) on a post-ganglionic axon (P). Note, a subsynaptic bar is present below the vacated site.

*B*, a vacated synaptic site (arrow) on the neuronal perikaryon (C). Glial processes (G) cover the post-ganglionic cell, including the vacated site.

Electron micrographs of regenerating vagal synapses in the cardiac ganglion.

*C*, a regenerated, axo-axonic synapse, 4 weeks after bilateral vagotomy. A varicosity in the vagal preganglionic terminal (V) forms a synaptic contact with the post-ganglionic axon (P).

*D*, vagal reinnervation of the cell body 7 weeks after crushing the cardiac vagus nerve branches. A vagal bouton (V) contacts the perikaryon (C). Glial processes (G) cover the cell body, including the vagal bouton.

Calibrations, *A*, *B* = 0.5  $\mu$ m; *C*, *D* = 1  $\mu$ m.